

# Undiscovered pulsar in the Local Bubble as an explanation of the local high energy cosmic ray all-electron spectrum

R. López-Coto,<sup>1,2,\*</sup> R.D. Parsons,<sup>2</sup> J.A. Hinton,<sup>2</sup> and G. Giacinti<sup>2</sup>

<sup>1</sup>*INFN and Università di Padova, I-35131, Padova, Italy*

<sup>2</sup>*Max-Planck-Institut für Kernphysik, P.O. Box 103980, D 69029 Heidelberg, Germany*

(Dated: March 16, 2022)

Cosmic ray electrons and positrons are tracers of particle propagation in the interstellar medium (ISM). A recent measurement performed using H.E.S.S. extends the all-electron (electron+positron) spectrum up to 20 TeV, probing very local sources and transport due to the  $\sim 10$  kyr cooling time of these particles. An additional key local measurement was the recent estimation of the ISM diffusion coefficient around Geminga performed using HAWC. The inferred diffusion coefficient is much lower than typically assumed values. It has been argued that if this diffusion coefficient is representative of the local ISM, pulsars would not be able to account for the all-electron spectrum measured at the Earth. Here we show that a low diffusion coefficient in the local ISM is compatible with a pulsar wind nebula origin of the highest energy electrons, if a so far undiscovered pulsar with spin-down power  $\sim 10^{33-34}$  erg/s exists within 30 to 80 pc of the Earth. The existence of such a pulsar is broadly consistent with the known population and may be detected in near future survey observations.

## INTRODUCTION

The measured cosmic ray spectrum at the Earth is dominated by protons and nuclei, with a much smaller fraction of electrons and positrons. The electron spectrum is dominated by primary cosmic rays accelerated inside sources as supernova remnants or pulsar wind nebulae. The positron spectrum, at least below energies of  $\sim 10$  GeV, is dominated by secondary production in cosmic-ray collisions in the interstellar medium (ISM). Electrons and positrons suffer severe energy losses due to interstellar magnetic and radiation fields [1]. That the local all-electron spectrum (LAES hereafter) provides information about very local sources and might contain a large positron fraction at high energies, has long been recognized [1, 2]. Nevertheless, the detection of an increasing positron fraction at the highest energies [3–5] has led to intense speculation on their origin. This positron excess (over expected secondary production) has been postulated to arise from pulsar wind nebulae [2, 6], microquasar jets [7] or dark matter annihilation [8]. According to the most commonly accepted propagation theories within the ISM, the highest-energy positrons measured by satellites ( $\sim 500$  GeV) must originate from a region within  $\sim 1$  kpc from the Earth, limiting the number of possible sources producing this excess [2].

Recent measurements of the LAES demonstrate the existence of very local sources of high energy electrons. H.E.S.S. [9] presented a preliminary measurement of the LAES extending up to  $\sim 20$  TeV with a break at  $\sim 900$  GeV, later confirmed by DAMPE [10] and CALET [11]. Furthermore, the HAWC collaboration has recently reported the diffusion coefficient inferred from the VHE  $\gamma$ -ray measurements of the Geminga region [12]. The energy-dependent diffusion coefficient is usually characterized as  $D(E) = D_0(E/10\text{GeV})^\delta$ . The HAWC inferred value is  $D(100\text{ TeV}) = 4.5 \times 10^{27} \text{ cm}^2/\text{s}$ , which assuming

diffusion in Kolmogorov turbulence  $\delta = 0.33$  this implies  $D_0 \sim 2 \times 10^{26} \text{ cm}^2/\text{s}$ . This is two orders of magnitude lower than the average of the ISM derived from Galactic propagation codes fitting primary and secondary species spectra, see e.g. [13]. They argue that the diffusion coefficient measured does not need to be limited to the region surrounding Geminga, but may be characteristic of the local ISM. It has been argued that if this is indeed the case, the LAES could not be explained by known nearby pulsars [14].

Whilst the GeV electron spectrum in the ISM must include contributions from a whole population of sources across the Galaxy, at energies of many TeV it becomes increasingly likely that a single source dominates. A low diffusion coefficient exacerbates this problem, confining electrons to a smaller region around their sources within their cooling time. Figure 1 explores this effect quantitatively using a simple population model from the *gammapy* package [15] assuming a supernova rate of 3 per century. These sources were distributed using the radial distribution described in [16] with the velocity distribution and spiral arms used by [17]. The maximum fraction of the locally measured all electron flux contributed by a single source is shown for three different diffusion coefficients over 1000 realizations of the Galaxy. Sources are simulated with a pulsar-like evolution (described in detail later) and simplified particle propagation neglecting the Klein-Nishina effect in the inverse Compton losses [1]. As expected the highest energies are dominated by a small number of sources due to cooling effects. The energy at which a single source dominates shifts to lower values for lower diffusion coefficients. With the typically used diffusion coefficient of  $D_0 = 10^{28} \text{ cm}^2\text{s}^{-1}$  a single source dominates the spectrum in almost all realizations above 2 TeV. With a diffusion coefficient of  $D_0 = 10^{26} \text{ cm}^2\text{s}^{-1}$  a single source may dominate as early as 100 GeV.

Here we argue that even in slow diffusion scenarios

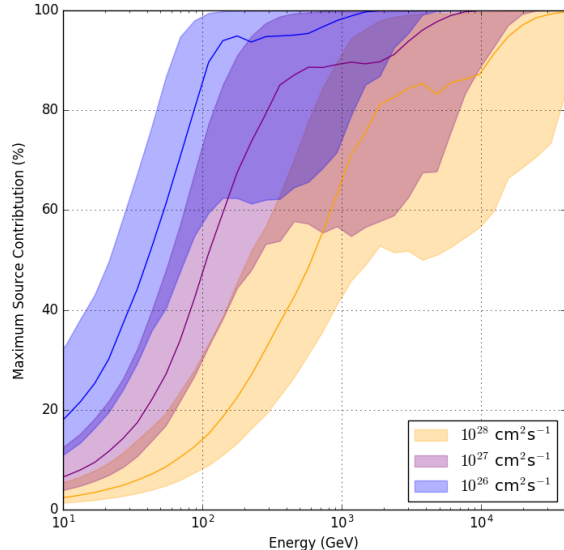


FIG. 1. Maximum contribution of a single source to the total cosmic ray electron spectrum as a function of energy for three diffusion coefficients with an energy dependence of  $\delta = 0.33$ . Generated from 1000 realizations of a source population and simple propagation model. Solid lines correspond to the median of the distribution and the bands correspond to the 16<sup>th</sup> and 84<sup>th</sup> percentiles.

a single pulsar wind nebula (PWN) explanation of the high energy LAES remains plausible. We estimate the required parameters for the pulsar powering such a PWN, its consistency with the known population and the likelihood that it could remain undetected.

### APPROACH

We use `edge`, a code that calculates the isotropic diffusion of electrons from a point source [18] to compute the LAES produced by the considered source. The code computes the solution of the diffusion-loss equation using the quasi-analytical result put forward in [1]. The time-dependence of the electron injection is given by the assumption that the power source is a pulsar and its luminosity evolution is given by:  $\dot{E}(t) = \dot{E}_0 \left(1 + \frac{t}{\tau_0}\right)^{-\frac{n+1}{n-1}}$  where  $n$  is the braking index of the pulsar and  $\dot{E}_0$  the initial luminosity.  $\tau_0$  is the initial spin-down timescale of the pulsar and is related to the initial birth period of the pulsar  $P_0$ , the current period ( $P$ ) and the characteristic age ( $\tau_c$ ) by:  $(P/P_0)^{n-1} = 2\tau_c/\tau_0(n-1)$ . For this work we assume a  $\tau_c=342$  kyr and a  $P = 237$  ms as in the Geminga pulsar and hence  $\tau_0$  is a function of the assumed  $P_0$ . We use  $P_0=40$  ms, corresponding to  $\tau_0 = 10^4$  yr. The spin-down power simulated is  $\dot{E} = 3.2 \times 10^{34}$

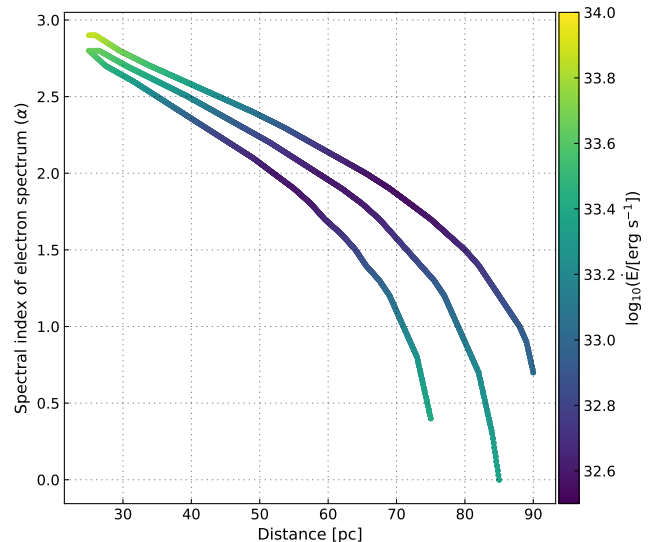


FIG. 2. Required spectral index  $\alpha$  vs pulsar distance for different magnetic fields (top line:  $B = 3\mu\text{G}$ , middle line:  $B = 4\mu\text{G}$ , bottom line:  $B = 5\mu\text{G}$ ). The color scale gives the energy into accelerated electrons needed to match the local electron flux in the range 1–20 TeV as measured by H.E.S.S..

erg/s.

We consider that electrons and positrons are injected into the ISM from a pulsar wind nebula (PWN) with a power-law spectrum  $dN/dE = f_0 E^{-\alpha}$  as appears to be the case for Geminga [12] and as may be the case in general for sufficiently old systems. For the particle propagation we only consider diffusion with the normalization measured by HAWC  $D_0 = 2 \times 10^{26} \text{ cm}^2 \text{ s}^{-1}$  and the energy-dependence  $\delta=0.33$  corresponding to an ISM dominated by Kolmogorov turbulence. Assuming a larger  $\delta$  would imply faster propagation and the best fit results would be shifted, but the dominant effect will be that of the spectral index of the electrons  $\alpha$ . We assume a typical magnetic field in the ISM of  $B = 3\mu\text{G}$  and photon energy densities for Cosmic Microwave Background (CMB), infrared (IR) and optical radiation fields of  $\epsilon_{\text{CMB}}=0.26 \text{ eV/cm}^{-3}$ ,  $\epsilon_{\text{IR}}=0.3 \text{ eV/cm}^{-3}$ ,  $\epsilon_{\text{Opt}}=0.3 \text{ eV/cm}^{-3}$  for the photon targets, which are the typical values derived by GALPROP for the location of Geminga [19]. The magnetic field in the nearby ISM should be in the range between 3-5  $\mu\text{G}$  according to [20]. We take into account losses due to ionization, bremsstrahlung, synchrotron and inverse Compton in the Klein-Nishina regime.

### CHARACTERISTICS OF A SINGLE SOURCE

Under the assumptions and calculation method given above we explore the available pulsar parameters in an

attempt to match the observed LAES at TeV energies for a single source and a slow diffusion coefficient. The following are the free parameters of the fit with their allowed ranges:

- Distance ( $25 \text{ pc} < d < 100 \text{ pc}$ )
- Spectral index of injected electrons ( $0 < \alpha < 3$ )

The characteristic age  $\tau_c$  is not a critical parameter if the equilibrium where all electrons in the 1–20 TeV regime are already cooled has been reached. Therefore, for sources with age  $\gtrsim 300 \text{ kyr}$  this parameter does not affect the measurements (see Figure 11 of [18]). For younger pulsars, they could not account for all the LAES above 1 TeV as it is required for this diffusion coefficient by Figure 1. Hence for this study we fix  $\tau_c$  to the 342 kyr value of Geminga [21]. The amount of energy into electrons is derived by normalization to the measured flux (see below).

After calculating the LAES for a grid of the parameters in the ranges above, we fit the spectrum between 1 and 20 TeV using a single power-law and choose for each distance the  $\alpha$  that produces the closest spectral index to that measured by H.E.S.S. in the same energy range. We consider three different magnetic field strengths ( $B = 3, 4$  and  $5 \mu\text{G}$ ) to investigate the dependence on synchrotron losses. The results for the best fit values for every pair of  $d - \alpha$  are shown in Figure 2. For every pair of values, the best fit requires a different energy into electrons  $\mu \dot{E}$  to fit H.E.S.S. data in this energy range. Here  $\mu$  is the fraction of the total spin-down power that is transformed into electrons. The relationship between distance and predicted slope, and hence the requirement for a different injection index, is illustrated in [18]. Contrary to intuition, nearby sources require a higher spin-down power than more distant ones. This is the result of requiring a much softer spectral index for the injected electrons for close-by sources to reproduce the H.E.S.S. spectral index, which implies fewer electrons injected at high energies. At some distance that depends on the magnetic field strength assumed, the distance dominates again over the softening of the spectrum and the  $\dot{E}$  increases again. We find that the pulsar producing the LAES between 1 and 20 TeV should be located between 25–80 pc, with an  $\dot{E}$  of  $10^{33-34} \text{ erg/s}$ , with effectively no constraint on the injection spectral index. The different magnetic fields considered do not significantly change the conclusion.

In Figure 3, we show the LAES for different  $P_0$  values for the example of a pulsar located at 50 pc, with corresponding best fit values of  $\alpha=2.4$  and  $\dot{E} = 1.3 \times 10^{33} \text{ erg/s}$ . The overall shape of the spectrum at TeV energies is consistent, but it is clear that short initial periods ( $P_0 \lesssim 140 \text{ ms}$ ) overshoot the measured LAES at low energies. However, as discussed in [18], those parameters relating to the early evolution of the pulsar ( $\tau_0$ ,  $n$  and  $P_0$ ) have a large effect on the prediction in the energy

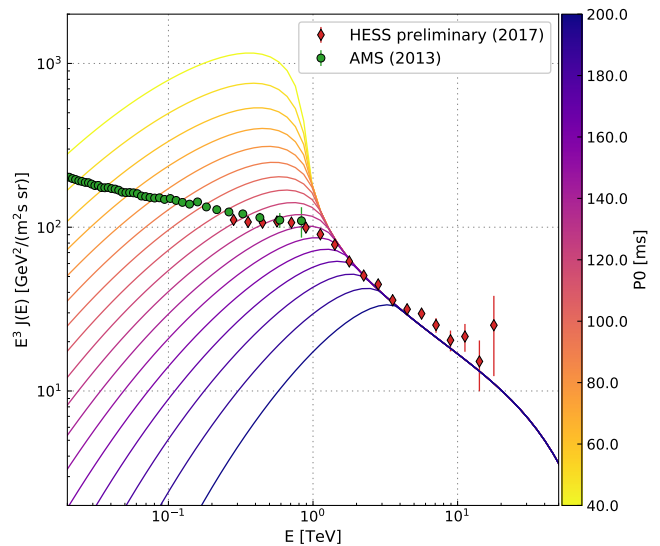


FIG. 3. All electron spectrum measured at the Earth with AMS [22] and preliminary H.E.S.S. [9] data points compared to predictions for a single PWN. The colored lines correspond to the LAES contribution of a single pulsar located at 50 pc,  $\dot{E} = 1.3 \times 10^{33} \text{ erg/s}$ ,  $\alpha = 2.4$ , an ISM magnetic field of  $B = 3 \mu\text{G}$  and a range of values for  $P_0$ .

range where the spectrum is uncooled. For the assumed source age and slow diffusion this occurs below  $\simeq 1 \text{ TeV}$ . We note that the assumption of escape without losses becomes increasingly questionable in the early life of a PWN and hence the lowest energy predictions can be seen as upper limits. At higher energies however evolutionary uncertainties are less critical and in the TeV range the single source predictions are more robust. Furthermore, below 1 TeV multiple sources may contribute and a population model is needed to predict the resulting LAES. The requirement for the single source model is therefore consistency with the LAES at TeV energies and to not overshoot the total  $e^+$  and  $e^-$  fluxes at lower energies. Birth periods greater than  $\sim 160 \text{ ms}$  are therefore disfavored as they do not produce sufficient flux around 2 TeV.

Figure 4 shows the measured positron fraction and predictions from the single source model. We assume that equal fluxes of electrons and positrons are injected by the hypothetical nearby PWN and a contribution from secondary positrons following [19]. As for Figure 3 curves for different values of the pulsar birth period  $P_0$  are shown. Short birth periods ( $P_0 \lesssim 140 \text{ ms}$ ) are again formally excluded, but as discussed above this constraint is readily avoided by considering significant losses before escape for those electrons accelerated in the early life of the PWN.

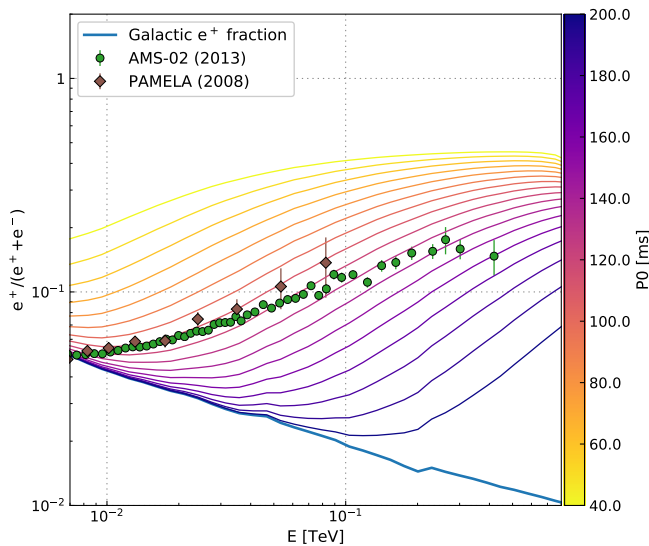


FIG. 4. Positron fraction measured at the Earth using AMS [23] and PAMELA [24]. The blue solid line corresponds to the predicted positron fraction due to secondary production from [19]. The colored lines correspond to the positron fraction with this level of secondaries plus a single PWN as for Figure 3.

As Figure 1 illustrates, more than one pulsar is expected to contribute to the LAES and therefore to the positron fraction at energies below hundreds of GeV. However the dominance of a single PWN at high energies necessitates a further rise in the positron fraction beyond the range of current measurements ultimately reaching 0.5, and indeed this is the case for any PWN-dominated model.

The final observational constraint that we consider is the anisotropy of the all-electron flux. Using the LAES, its gradient and the diffusion coefficient, we calculate the anisotropy using equation 3.2 of [25]. We show the result for curves with a range of  $P_0$  that is consistent with the previous constraints. Figure 5 shows the resulting predictions together with the upper limits established from *Fermi-LAT* [26].

We note that the conclusions of required birth periods are somewhat modified for values of distance and ISM magnetic field differing from the 50 pc and  $3 \mu\text{G}$  assumptions made for Figures 3, 4 and 5. However, as Figure 2 shows, solutions exist for a range of distances and magnetic fields provided appropriate choices are made for injected electron spectral index and injection power.

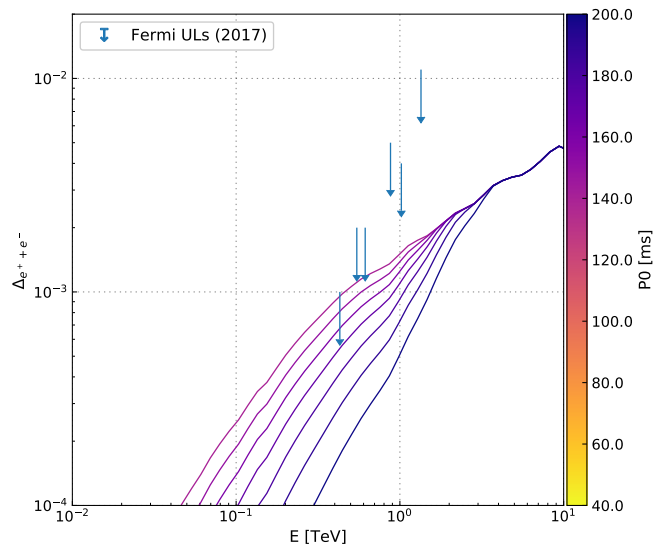


FIG. 5. Expected anisotropy due to the single local source simulated in Figures 3 and 4. Fermi upper limits are shown as blue arrows. The color code for the single pulsar contribution is the same as on the aforementioned figures.

## DISCUSSION

As shown in the previous section the high energy LAES can plausibly be explained by particle acceleration in a single PWN only if it is very local (within  $\sim 80$  pc) more than  $\sim 3 \times \sim 10^5$  years old and with  $\dot{E} \sim 10^{33-34}$  erg/s. The measured  $\dot{E}/\text{age}$  relationship [21] suggests that such  $\dot{E}$  values are common for pulsars of around Myr age. To assess the likelihood of the existence of such a local pulsar we used the source population simulations introduced earlier. These population simulations predict a pulsar within 80 pc in around 5-10% of the realizations. The existence of such a pulsar implies the occurrence of a recent local supernova, the case for which is strengthened by studies of  $^{60}\text{Fe}$  transport [27, 28]. By modeling the formation of the Local Bubble by several supernovae they find that the most recent supernovae must have exploded at a distance of 90-100 pc from the Earth, 2-3 Myr ago with a suitable initial mass to produce a pulsar [29].

No known pulsar exists with the properties required. However, the beam fraction of a pulsar is a quite uncertain value and in many cases, for example [30], is predicted to be rather small ( $< 25\%$ ), in particular for old pulsars. Beaming could potentially lead to a number of pulsars in the local neighborhood which are undetectable by radio observations. These objects, however with their surface temperature of a few million Kelvin may be de-

tectable in soft X-rays by a wide field of view instrument, as for the "Magnificent seven" local neutron stars discovered using ROSAT (for example [31, 32]). Again no candidate sources have been detected within 100 pc, but confirmation and distance measurements of these sources remains difficult due to their often weak optical counterparts. X-ray measurements of a synchrotron pulsar wind nebula as in the case of Geminga [33] would also be a way of detecting them, but we note that the X-ray detection of Geminga relied on the early detection of pulsed emission. VHE  $\gamma$ -ray observations provide an alternative method for detecting PWN and electrons around them (see e.g. [12, 34, 35]). Assuming a source powered by a central pulsar with spin-down power  $10^{34}$  erg/s, the VHE  $\gamma$ -ray flux within  $5^\circ$  is more than one order of magnitude lower than that measured by HAWC for Geminga and therefore out of the reach of current or planned VHE facilities.

### SUMMARY

We have shown that even with the two orders of magnitude lower diffusion coefficient than the conventional expectation inferred from Geminga using HAWC, a single local pulsar wind nebula remains as a feasible source of the highest energy cosmic ray electrons. The required properties of the pulsar powering this nebula are an  $\dot{E} \sim 10^{33-34}$  erg/s and an age of  $>300$  kyr, at a distance of 30–80 pc. Population modeling suggests a probability for the existence of such a pulsar is of order 10% for an age  $<1$  Myr. The probability of missing such a pulsar in existing surveys may be rather large due to the beaming fraction of old pulsars and the low surface brightness of the associated VHE  $\gamma$ -ray nebula. If such a pulsar exists there are good prospects for its discovery in future surveys at (for example) radio or X-ray wavelengths.

### REFERENCES

- 
- \* rlopez@pd.infn.it
- [1] Atoyan, A. M., et al., Electrons and positrons in the galactic cosmic rays, *Phys. Rev. D* 52 (1995) 3265–3275. doi:10.1103/PhysRevD.52.3265.
  - [2] Aharonian, F. A., et al., High energy electrons and positrons in cosmic rays as an indicator of the existence of a nearby cosmic tevatron, *A&A* 294 (1995) L41–L44.
  - [3] Adriani, O., et al., An anomalous positron abundance in cosmic rays with energies 1.5–100 GeV, *Nature (London)* 458 (2009) 607–609. arXiv:0810.4995, doi:10.1038/nature07942.
  - [4] Ackermann, M., et al., Measurement of Separate Cosmic-Ray Electron and Positron Spectra with the Fermi Large Area Telescope, *Physical Review Letters* 108 (1) (2012) 011103. arXiv:1109.0521, doi:10.1103/PhysRevLett.108.011103.
  - [5] Aguilar, M., et al., First Result from the Alpha Magnetic Spectrometer on the International Space Station: Precision Measurement of the Positron Fraction in Primary Cosmic Rays of 0.5–350 GeV, *Physical Review Letters* 110 (14) (2013) 141102. doi:10.1103/PhysRevLett.110.141102.
  - [6] Hooper, D., et al., Pulsars as the sources of high energy cosmic ray positrons, *JCAP* 1 (2009) 025. arXiv:0810.1527, doi:10.1088/1475-7516/2009/01/025.
  - [7] Gupta, N. et al.,  $p\gamma$  interactions in Galactic jets as a plausible origin of the positron excess, *MNRAS* 441 (2014) 3122–3126. arXiv:1404.4188, doi:10.1093/mnras/stu770.
  - [8] Bergström, L., et al., New positron spectral features from supersymmetric dark matter: A way to explain the PAMELA data?, *Phys. Rev. D* 78 (10) (2008) 103520. arXiv:0808.3725, doi:10.1103/PhysRevD.78.103520.
  - [9] Kerszberg, D. (for the H. E. S. S. Collaboration), The cosmic-ray electron spectrum measured with H.E.S.S., *International Cosmic Ray Conference, [CR1215]* (2017).
  - [10] DAMPE Collaboration, et al., Direct detection of a break in the teraelectronvolt cosmic-ray spectrum of electrons and positrons, *Nature (London)* 552 (2017) 63–66. arXiv:1711.10981, doi:10.1038/nature24475.
  - [11] Adriani, O., et al., Energy Spectrum of Cosmic-Ray Electron and Positron from 10 GeV to 3 TeV Observed with the Calorimetric Electron Telescope on the International Space Station, *Physical Review Letters* 119 (18) (2017) 181101. arXiv:1712.01711, doi:10.1103/PhysRevLett.119.181101.
  - [12] Abeysekara, A. U., et al., Extended gamma-ray sources around pulsars constrain the origin of the positron flux at Earth, *Science* 358 (2017) 911–914. doi:10.1126/science.aan4880.
  - [13] Amato, E. et al., Cosmic Ray Transport in the Galaxy: a Review, *ArXiv e-prints* arXiv:1704.05696.
  - [14] Hooper, D. et al., Measuring the Local Diffusion Coefficient with H.E.S.S. Observations of Very High-Energy Electrons, *ArXiv e-prints* arXiv:1711.07482.
  - [15] Deil, C., et al., Gammapy - A prototype for the CTA science tools, *ArXiv e-prints* (2017) arXiv:1709.01751 arXiv:1709.01751.
  - [16] Lorimer, D. R., et al., The Parkes Multibeam Pulsar Survey - VI. Discovery and timing of 142 pulsars and a Galactic population analysis, *MNRAS* 372 (2006) 777–800. arXiv:astro-ph/0607640, doi:10.1111/j.1365-2966.2006.10887.x.
  - [17] Faucher-Giguère, C.-A. et al., Birth and Evolution of Isolated Radio Pulsars, *Astrophys. J.* 643 (2006) 332–355. arXiv:astro-ph/0512585, doi:10.1086/501516.
  - [18] López-Coto, R., et al., Effect of the diffusion parameters on the observed gamma-ray spectrum of sources and their contribution to the local all-electron spectrum: the EDGE code, *ArXiv e-prints* arXiv:1709.07653.
  - [19] Moskalenko, I. V. et al., Production and Propagation of Cosmic-Ray Positrons and Electrons, *Astrophys. J.* 493 (1998) 694–707. arXiv:astro-ph/9710124, doi:10.1086/305152.
  - [20] López-Coto, R. et al., Constraining the properties of the magnetic turbulence in the Geminga region using HAWC  $\gamma$ -ray data, *ArXiv e-prints* arXiv:1712.04373.

- [21] Manchester, R. N., et al., The Australia Telescope National Facility Pulsar Catalogue, *AJ*129 (2005) 1993–2006. [arXiv:astro-ph/0412641](#), [doi:10.1086/428488](#).
- [22] Aguilar, M., et al., Electron and Positron Fluxes in Primary Cosmic Rays Measured with the Alpha Magnetic Spectrometer on the International Space Station, *Physical Review Letters* 113 (12) (2014) 121102. [doi:10.1103/PhysRevLett.113.121102](#).
- [23] Accardo, L., et al., High Statistics Measurement of the Positron Fraction in Primary Cosmic Rays of 0.5-500 GeV with the Alpha Magnetic Spectrometer on the International Space Station, *Physical Review Letters* 113 (12) (2014) 121101. [doi:10.1103/PhysRevLett.113.121101](#).
- [24] Adriani, O., et al., An anomalous positron abundance in cosmic rays with energies 1.5-100GeV, *Nature (London)*458 (2009) 607–609. [arXiv:0810.4995](#), [doi:10.1038/nature07942](#).
- [25] Manconi, S., et al., Dipole anisotropy in cosmic electrons and positrons: inspection on local sources, *JCAP*1 (2017) 006. [arXiv:1611.06237](#), [doi:10.1088/1475-7516/2017/01/006](#).
- [26] Abdollahi, S., et al., Search for Cosmic-Ray Electron and Positron Anisotropies with Seven Years of Fermi Large Area Telescope Data, *Physical Review Letters* 118 (9) (2017) 091103. [arXiv:1703.01073](#), [doi:10.1103/PhysRevLett.118.091103](#).
- [27] Kachelrieß, M., et al., Signatures of a Two Million Year Old Supernova in the Spectra of Cosmic Ray Protons, Antiprotons, and Positrons, *Physical Review Letters* 115 (18) (2015) 181103. [arXiv:1504.06472](#), [doi:10.1103/PhysRevLett.115.181103](#).
- [28] Schulreich, M. M., et al., Numerical studies on the link between radioisotopic signatures on Earth and the formation of the Local Bubble. I.  $^{60}\text{Fe}$  transport to the solar system by turbulent mixing of ejecta from nearby supernovae into a locally homogeneous interstellar medium, *A&A*604 (2017) A81. [arXiv:1704.08221](#), [doi:10.1051/0004-6361/201629837](#).
- [29] Breitschwerdt, D., et al., The locations of recent supernovae near the Sun from modelling  $^{60}\text{Fe}$  transport, *Nature (London)*532 (2016) 73–76. [doi:10.1038/nature17424](#).
- [30] Tauris, T. M. et al., On the Evolution of Pulsar Beams, *MNRAS*298 (1998) 625–636. [doi:10.1046/j.1365-8711.1998.01369.x](#).
- [31] Walter, F. M., et al., Discovery of a nearby isolated neutron star, *Nature (London)*379 (1996) 233–235. [doi:10.1038/379233a0](#).
- [32] Zampieri, L., et al., 1RXS J214303.7+065419/RBS 1774: A new Isolated Neutron Star candidate, *A&A*378 (2001) L5–L9. [arXiv:astro-ph/0108456](#), [doi:10.1051/0004-6361:20011151](#).
- [33] Caraveo, P. A., et al., Geminga’s Tails: A Pulsar Bow Shock Probing the Interstellar Medium, *Science* 301 (2003) 1345–1348. [doi:10.1126/science.1086973](#).
- [34] H. E. S. S. Collaboration, et al., The population of TeV pulsar wind nebulae in the H.E.S.S. Galactic Plane Survey, *A&A*612 (2018) A2. [arXiv:1702.08280](#), [doi:10.1051/0004-6361/201629377](#).
- [35] Linden, T., et al., Using HAWC to discover invisible pulsars, *Phys. Rev. D*96 (10) (2017) 103016. [arXiv:1703.09704](#), [doi:10.1103/PhysRevD.96.103016](#).